

# Use of positron emission tomography-computed tomography to predict axillary metastasis in patients with triple-negative breast cancer

Jung Hyun Youm<sup>1</sup>, Yoona Chung<sup>1</sup>, You Jung Yang<sup>2</sup>, Sang Ah Han<sup>1</sup>, Jeong Yoon Song<sup>1</sup>

Departments of <sup>1</sup>Surgery and <sup>2</sup>Nuclear Medicine, Kyung Hee University Hospital at Gangdong, Seoul, Korea

**Purpose:** Axillary lymph node dissection (ALND) and sentinel lymph node biopsy (SLNB) are important for staging of patients with node-positive breast cancer. However, these can be avoided in select micrometastatic diseases, preventing postoperative complications. The present study evaluated the ability of axillary lymph node maximum standardized uptake value (SUVmax) on positron emission tomography-computed tomography (PET-CT) to predict axillary metastasis of breast cancer.

**Methods:** The records of invasive breast cancer patients who underwent pretreatment (surgery and/or chemotherapy) PET-CT between January 2006 and December 2014 were reviewed. ALNs were preoperatively evaluated by PET-CT. Lymph nodes were dissected by SLNB or ALND. SUVmax was measured in both the axillary lymph node and primary tumor. Student t-test and chi-square test were used to analyze sensitivity and specificity. Receiver operating characteristic (ROC) and area under the ROC curve (AUC) analyses were performed.

**Results:** SUV-tumor (SUV-T) and SUV-lymph node (SUV-LN) were significantly higher in the triple-negative breast cancer (TNBC) group than in other groups (SUV-T: 5.99,  $P < 0.01$ ; SUV-LN: 1.29,  $P = 0.014$ ). The sensitivity (0.881) and accuracy (0.804) for initial ALN staging were higher in fine needle aspiration+PET-CT than in other methods. For PET-CT alone, the subtype with the highest sensitivity (0.870) and negative predictive value (0.917) was TNBC. The AUC for SUV-LN was greatest in TNBC (0.797).

**Conclusion:** The characteristics of SUV-T and SUV-LN differed according to immunohistochemistry subtype. Compared to other subtypes, the true positivity of axillary metastasis on PET-CT was highest in TNBC. These findings could help tailor management for therapeutic and diagnostic purposes.

**Keywords:** Breast neoplasms, Triple negative breast neoplasms, Lymphatic metastasis, Positron emission tomography computed tomography, ROC curve

## INTRODUCTION

Breast cancer is the most common type of invasive cancer among

Received: Sep 29, 2018 Revised: Oct 18, 2018 Accepted: Oct 22, 2018

Correspondence to: Sang Ah Han

Department of Surgery, Kyung Hee University Hospital at Gangdong, 892 Dongnam-ro, Gangdong-gu, Seoul 05278, Korea

Tel: +82-2-440-6241, Fax: +82-2-440-8197

E-mail: ivory521@naver.com

ORCID: Jung Hyun Youm (<https://orcid.org/0000-0001-5368-0191>), Yoona Chung (<https://orcid.org/0000-0002-2812-8714>), You Jung Yang (<https://orcid.org/0000-0001-7345-7536>), Sang Ah Han (<https://orcid.org/0000-0001-6629-955X>), Jeong Yoon Song (<https://orcid.org/0000-0002-2269-1055>)

Copyright © 2018 Korean Society of Surgical Oncology

This is an Open Access article distributed under the terms of the Creative Commons Attribution Non-Commercial License (<http://creativecommons.org/licenses/by-nc/4.0>) which permits unrestricted non-commercial use, distribution, and reproduction in any medium, provided the original work is properly cited.

women and is the second leading cause of cancer-related death. The diagnosis of breast cancer is based on clinical examination combined with imaging and is confirmed by histopathological assessment. Imaging includes bilateral mammography and ultrasonography of the breast and regional lymph nodes (LNs).

Axillary lymph node (ALN) metastasis is an important prognostic factor, and the diagnosis of ALN metastasis is essential for treatment planning, such as start of neoadjuvant chemotherapy or selection of a neoadjuvant chemotherapy agent [1-4].

Although ALN dissection is the standard method of staging in breast cancer, it is associated with postoperative morbidities, such as arm and shoulder pain, lymphedema, paresthesia, nerve injuries, and seroma [5,6]. Sentinel LN biopsy, a less-invasive procedure, is also being used for breast cancer staging, but its clinical application is limited to early-stage breast cancer with no clinical suspicion of ALN metastasis [7,8]. To overcome this limitation, imaging modal-

ities, such as mammography, ultrasonography, and computed tomography (CT), have been used to detect ALN metastasis, but unfortunately, their diagnostic accuracies are limited [9,10].

Fluorine-18 fluorodeoxyglucose ( $^{18}\text{F}$ -FDG) positron emission tomography-computed tomography (PET-CT) has been widely used for diagnosis, staging, treatment monitoring, and detection of disease recurrence in patients with breast cancer [11-13]. This technique has the advantage of being able to demonstrate abnormal metabolic activities associated with malignancy before the demonstration of abnormal morphological findings by anatomic imaging modalities. In addition, it can show the metabolic activity of the primary tumor and thus predict LN metastasis in various cancers especially non-small cell lung cancer [14].

However, breast cancer is comprised of biologically varying subtypes. Many previous studies have shown a good correlation between  $^{18}\text{F}$ -FDG uptake by primary tumor and molecular subtypes of breast cancer [15,16].

The aim of this study was to determine the ability of ALN maximum standardized uptake value (SUVmax) on PET-CT to predict axillary metastasis of breast cancer, and to correlate the results with ultrasonography and clinicopathologic findings.

## METHODS

### Patients

The records of breast cancer patients who had undergone PET-CT before receiving treatment (surgery and/or chemotherapy) for invasive breast carcinoma at Kyung Hee University Hospital at Gangdong between January 2006 and December 2014 were retrospectively collected and reviewed. The study was approved by the Institutional Review Board of Kyung Hee University Hospital at Gandong (IRB No. KHNMC 2018-10-016) and performed in accordance with the principles of the Declaration of Helsinki. The informed consent was waived. The axillary LNs were preoperatively evaluated by ultrasonography and PET-CT. Lymph nodes were removed by sentinel LN biopsy (SLNB) or axillary LN dissection (ALND) and were histologically diagnosed by experienced pathologists.

### Fine needle aspiration

All patients underwent routine preoperative ultrasonography. In cases with suspicious metastatic LNs (above the level of category 4a in the breast imaging-reporting and data system) on preoperative ultrasonography, fine needle aspiration (FNA) of the axilla was done [17].

### PET-CT and lymph node/tumor ratio

Whole-body PET-CT was performed within 1 month before treatment. All patients fasted at least 6 hours prior to the PET-CT pro-

cedure. After the serum glucose concentration was confirmed as  $< 150$  mg/dL, patients were administered 185 MBq of  $^{18}\text{F}$ -FDG intravenously in the arm or leg contralateral to the primary breast tumor and rested quietly for 60 minutes; they then underwent whole-body PET-CT, and the PET-CT images were reconstructed. The FDG uptake in the primary tumor (SUV-T) and lymph node (SUV-LN) was semi-quantitatively analyzed using the SUVmax, which was calculated based on the measured activity, decay-corrected administered dose, and patient weight. When calculating the SUV-LN, the ALN showing the highest SUV within the whole axillary space was selected. The lymph node/tumor (LN/T) ratio was calculated by dividing the SUV-LN by the SUV-T.

### Immunohistochemistry

Estrogen receptor (ER), progesterone receptor (PR), and human epidermal growth factor receptor 2 (HER2) expression were assessed by immunohistochemistry (IHC) using a polymer detection system with antibodies against these receptors. ER/PR expression was defined according to the Allred scoring system. The percentage of stained cells (scores, 0–5) and their intensity (scores, 0–3) were determined, and the sum of the intensity and percentage scores was calculated. Allred scores of 0 to 2 were defined as ER/PR negative, whereas scores of 3 to 8 were defined as ER/PR positive [18]. HER2/Erbb2 positivity was defined as an IHC score of 3+ or when the HER2 loci/chromosome 17 centromere ratio was  $> 2.2$ . The subtypes of breast cancer were defined as follows [19]: (1) luminal A: ER+ and/or PR+, HER2-, Ki-67 low ( $< 14\%$ ); (2) luminal B: ER+ and/or PR+, HER2-, and Ki-67 high ( $\geq 14\%$ ); (3) HER2+: ER-, PR-, and HER2+; or (4) triple-negative breast cancer (TNBC): ER-, PR-, and HER2-.

### Sentinel lymph node biopsy and axillary lymph node dissection

Each patient underwent either mastectomy or breast-conserving surgery based on the location and extension of the primary tumor. ALND was performed in patients with clinically positive ALNs, while in clinically node negative patients, SLNB was used for axillary evaluation [20]. At our institution, SLNB was performed using a dual-tracer technique, which is a combination of the blue dye method and the gamma probe-guided method. Imaging was performed 1 day preoperatively.

LN were categorized as suspicious if they exhibited one or more of the following characteristics: cortical thickening or eccentric cortical lobulation with obliteration of echogenic hilum, irregular shape, loss of fatty hilum, or round shape. Patients with pathologically FNA-positive nodes underwent ALND [10,17,21].

### Statistical analysis

Student t-test and the chi-square test were used to analyze the sen-

sitivity and specificity. Receiver operating characteristic (ROC) and area under the ROC curve (AUC) analyses were performed. The variables included in the analysis were enumerated. The included variables were mean age at surgery, tumor size, status of LN metastasis, SUV-LN, and SUV-T. SPSS version 18.0 (SPSS Inc., Chicago, IL, USA) was used for statistical analysis of intraclass correlation coefficient. All P-values less than 0.05 were considered statistically significant.

**Table 1.** Patient characteristics (n=348)

Characteristics	Value
Age (yr)	52.4 ± 11.3
Tumor size (cm)	2.33 ± 1.50
T stage	
T1	184 (52.9)
T2	144 (41.4)
T3	18 (5.2)
T4	2 (0.6)
N stage	
N0	225 (64.7)
N1	77 (22.1)
N2	33 (9.5)
N3	13 (3.7)
Stage	
IA	144 (41.4)
IIB	1 (0.3)
IIA	103 (29.6)
IIB	49 (14.1)
IIIA	36 (10.3)
IIIB	2 (0.6)
IIIC	13 (3.7)
ER	
Negative	105 (20.2)
Positive	243 (69.8)
PR	
Negative	139 (39.9)
Positive	209 (60.1)
Ki-67 status	
Low (< 14%)	187 (53.7)
High (≥ 14%)	161 (46.3)
HER2	
Negative	281 (80.7)
Positive	67 (19.3)
Subtype	
Luminal A	100 (28.7)
Luminal B	109 (31.3)
HER2	67 (19.3)
TNBC	72 (20.7)

Values are presented as mean ± standard deviation or number (%). ER, estrogen receptor; PR, progesterone receptor; HER2, human epidermal growth factor receptor 2; TNBC, triple-negative breast cancer.

## RESULTS

### Patient characteristics

The characteristics of the enrolled patients are detailed in Table 1. A total of 348 patients with operable, invasive breast cancer were enrolled, comprising 123 node-positive patients and 225 node-negative patients. The mean age was 52.4 years, and the mean tumor size was 2.33 cm. Patients were staged as follows: stage IA: 144 (41.4%); stage IB: one (0.3%); stage IIA: 103 (29.6%); stage IIB: 49 (14.1%); stage IIIA: 36 (10.3%); stage IIIB: two (0.6%); and stage IIIC: 13 (3.7%). The patients were divided into ER/PR+ low Ki-67: 100 (28.7%); ER/PR+ high Ki-67: 109 (31.3%); HER2+: 67 (19.3%); and TNBC: 72 (20.7%) according to IHC characteristics.

The mean age, surgery, and number of LN metastasis were not significantly different among the subtypes. However, tumor size (2.33 cm) was significantly higher in the HER2+ group (2.67 cm) than in other subtypes (P = 0.041) (Table 2).

### Prediction of lymph node metastasis by PET-CT and ROC curve analysis

Fig. 1 shows the ROC curves used for determining the optimal cutoff values of SUV axilla and the LN/T cutoff values of SUV-LN and LN/T ratio for the detection of ALN metastases. In the luminal A subtype, the AUC for SUV axilla was 0.617 (95% confidence interval [CI], 0.551–0.791) and the LN/T ratio was 0.668 (95% CI, 0.548–0.788). In the luminal B subtype, the AUC for SUV axilla was 0.685 (95% CI, 0.576–0.794) and the LN/T ratio was 0.689 (95% CI, 0.580–0.798). In the HER2+ subtype, the AUC for SUV axilla was 0.761 (95% CI, 0.640–0.882) and the LN/T ratio was 0.750 (95% CI, 0.672–0.873). In the TNBC subtype, the AUC for SUV axilla was 0.797 (95% CI, 0.688–0.907) and the LN/T ratio was 0.817 (95% CI, 0.711–0.923).

The mean SUV-T of the 348 tumors was 4.03 ± 3.33, and the mean SUV-LN was 0.92 ± 2.00. The corresponding mean SUV-T and SUV-LN are shown in the Table 2. The SUV-T and SUV-LN were significantly higher in the TNBC group than in the other groups (SUV-T: 5.99, P < 0.01; SUV-LN: 1.29, P = 0.014). However, there were no significant differences in the ratio of SUVmax. Metabolic semiquantitative parameters showed a significant correlation with molecular phenotype, with greater SUVs in more biologically aggressive tumors.

### Comparison of diagnostic performance

The sensitivity, specificity, positive predictive value (PPV), negative predictive value (NPV), and accuracy of the initial ALN staging were 0.831, 0.273, 0.671, 0.474, and 0.630 on FNA; 0.537, 0.853, 0.667, 0.771, and 0.741 on PET-CT; and 0.881, 0.667, 0.824, 0.757,

**Table 2.** The clinicopathologic findings of each group

Variable	Total (n = 348)	Luminal A (n = 100)	Luminal B (n = 109)	HER2+ (n = 67)	TNBC (n = 72)	P-value
Age at surgery (yr)	52.4 ± 11.3	51.9 ± 11.7	53.7 ± 11.5	51.5 ± 10.3	52.0 ± 11.2	0.610
Tumor size (cm)	2.33 ± 1.50	2.03 ± 1.46	2.33 ± 1.50	2.67 ± 1.76	2.42 ± 1.27	0.041
LN metastasis (n)	1.63 ± 4.43	1.26 ± 3.50	1.30 ± 2.56	2.09 ± 5.83	2.21 ± 6.03	0.152
SUVmax						
Breast	4.03 ± 3.33	2.81 ± 2.09	3.63 ± 2.70	4.41 ± 3.24	5.99 ± 4.58	<0.010
Axilla	0.92 ± 2.00	0.85 ± 2.37	0.49 ± 1.25	1.30 ± 2.47	1.29 ± 1.77	0.014
Ratio of SUVmax (axilla/breast)	0.32 ± 2.81	0.18 ± 0.48	0.11 ± 0.27	0.22 ± 0.37	0.93 ± 6.11	0.102

Values are presented as mean ± standard deviation.

HER2, human epidermal growth factor receptor 2; TNBC, triple-negative breast cancer; LN, lymph node; SUVmax, maximum standardized uptake value.

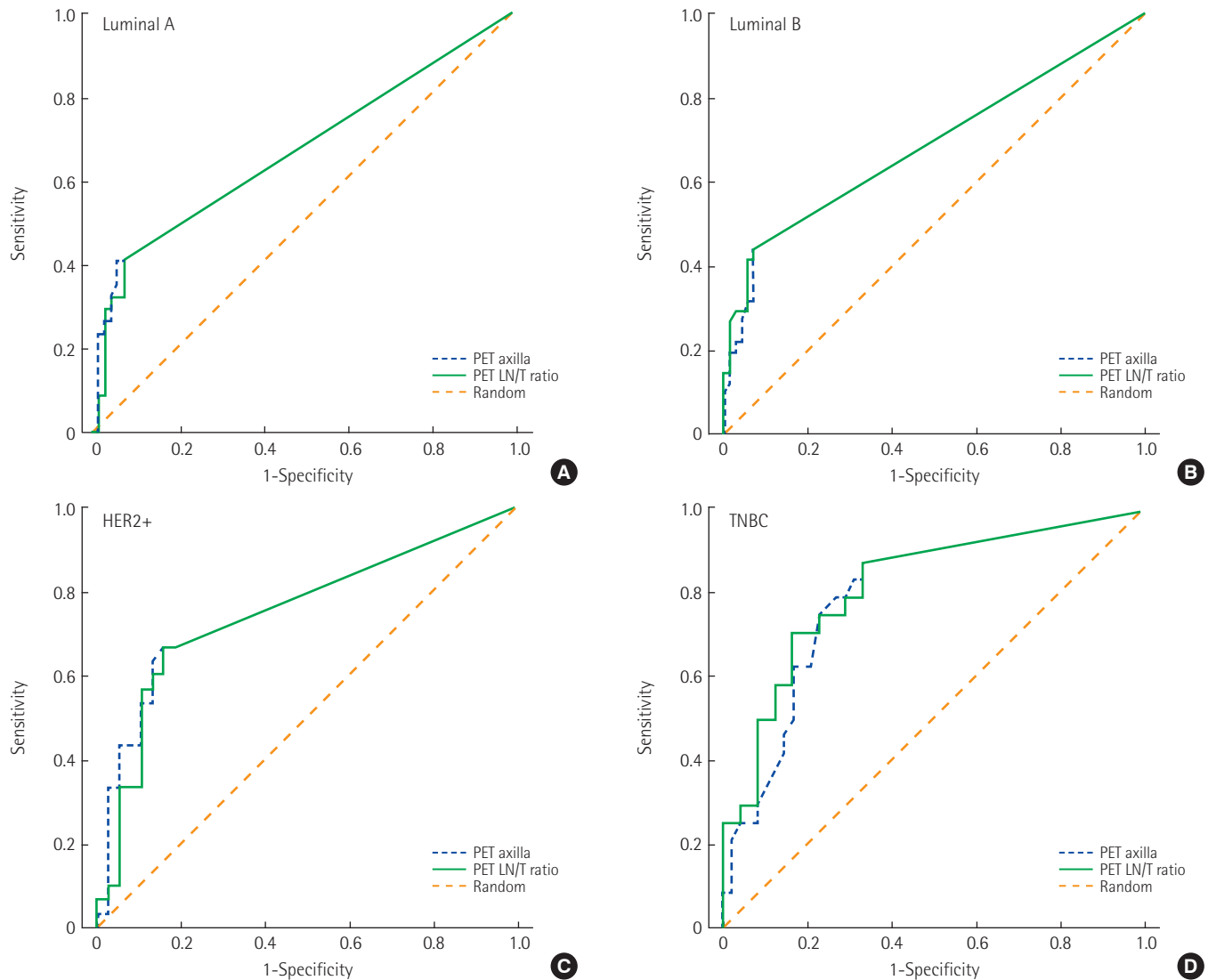


**Fig. 1.** Receiver operating characteristics curves for the lymph node/tumor (LN/T) ratio and standardized uptake value of the axillary lymph node. (A) Luminal A: PET axilla, 0.671; 95% confidence interval (CI), 0.551–0.791; PET LN/T ratio, 0.668; 95% CI, 0.548–0.788. (B) Luminal B: PET axilla, 0.685; 95% CI, 0.576–0.794; PET LN/T ratio, 0.689; 95% CI, 0.580–0.798. (C) HER2+: PET axilla, 0.761; 95% CI, 0.640–0.882; PET LN/T ratio, 0.750; 95% CI, 0.672–0.873. (D) TNBC: PET axilla, 0.797; 95% CI, 0.688–0.907; PET LN/T ratio, 0.817; 95% CI, 0.711–0.923. PET, positron emission tomography; HER2, human epidermal growth factor receptor 2; TNBC, triple-negative breast cancer.

**Table 3.** The predictive value of fine needle aspiration and SUVmax on PET-CT for metastatic axillary lymph nodes

Variable	FNA (n=99)	FNA+PET-CT (n=99)	PET-CT				
			Total (n=348)	Luminal A (n=100)	Luminal B (n=109)	HER2+ (n=67)	TNBC (n=72)
Sensitivity	0.831	0.881	0.537	0.364	0.410	0.643	0.870
Specificity	0.273	0.667	0.853	0.910	0.943	0.821	0.673
PPV	0.671	0.824	0.667	0.667	0.800	0.720	0.556
NPV	0.474	0.757	0.771	0.744	0.742	0.762	0.917
Accuracy	0.630	0.804	0.741	0.73	0.752	0.746	0.736
AUC			0.720	0.671	0.685	0.761	0.797

SUVmax, maximum standardized uptake value; PET-CT, positron emission tomography-computed tomography; FNA, fine needle aspiration; HER2, human epidermal growth factor receptor 2; TNBC, triple-negative breast cancer; PPV, positive predictive value; NPV, negative predictive value; AUC, area under the receiver operating characteristic curve.

and 0.804 on FNA+PET-CT, respectively. The sensitivity (0.881), PPV (0.824) and accuracy (0.804) for initial ALN staging were higher for FNA+PET-CT than for other methods.

In PET-CT alone, the subtype with the highest sensitivity (0.870) and NPV (0.917) was TNBC. The AUC of ROC curves for SUV-LN was greatest in TNBC (0.797) (Table 3).

## DISCUSSION

The major findings of the present study were that <sup>18</sup>F-FDG uptake by breast cancer, expressed as SUVmax, was significantly correlated with many clinicopathological features, and SUV-T and SUV-LN were significantly correlated with the molecular subtypes of breast cancer and were of value in predicting TNBC.

In the past, the treatment of choice for patients with newly diagnosed breast cancer was based on cancer size and presence of LN metastasis [22]. However, tumors in the same stage still comprise a heterogeneous group with different responses to treatment and different overall outcomes. Currently, biological features such as ER, PR, and HER2 status help predict prognoses and identify patients who are more likely to benefit from specific treatment.

Luminal A is the most common subtype of breast cancer, presenting a low expression of genes related to cellular proliferation. Patients with this subtype have a higher survival rate and lower relapse rate than patients with other subtypes because of the good response to hormone treatment [23].

The luminal B subtype has a more aggressive phenotype, higher histological grade, higher proliferative index, and worse prognosis compared to luminal A.

HER2+ breast cancers are characterized by a high expression of the *HER2* gene, which promotes tumor growth and progression [24]. They tend to be more aggressive than other subtypes; 75% have a high histological grade, more than 40% have p53 mutations, and they are less responsive to hormone treatment. The HER2+

subtype is clinically associated with a higher rate of recurrence and mortality due to tumor aggressiveness, although the advent of antibody treatment with trastuzumab targeting this receptor has improved survival outcomes in the last decade.

TNBC has a more aggressive biology than other subtypes, is associated with a poor outcome compared to the luminal subtypes [25], and no form of targeted therapy has yet been developed. Basu et al. [26] demonstrated that TNBCs were associated with higher FDG uptake than ER+, PR+, and HER2- tumor, and thus concluded that the enhanced FDG uptake of TNBC is likely related to its aggressive biology.

Various imaging modalities have been used for ALN staging in breast cancer, but the limited diagnostic accuracies have prevented the replacement of surgical ALN staging. Mammography is affected by technique and positioning [27], and the reported sensitivity of mammography and CT for ALN metastasis is low, ranging from 30% to 40% and 50%, respectively [28]. Ultrasonography has been widely used for staging breast cancer, but results are examiner dependent [29], and the reported sensitivity and specificity of ultrasonography for ALN metastasis vary from 49% to 87% and from 56% to 97%, respectively [10]. These imaging modalities primarily depend on LN size or shape for the differentiation of metastatic and nonmetastatic LNs. Therefore, normal or small-size metastatic LNs can be easily missed. Furthermore, the variable morphologic characteristics of LN also reduce accuracy because of the overlapping features of metastatic and nonmetastatic LN [29,30].

SUVmax, a semiquantitative metabolic parameter obtained by <sup>18</sup>F-FDG PET-CT, was found to be significantly correlated with the molecular subtype of breast cancer, higher values being evident in more biologically aggressive tumors.

The limited diagnostic performances of PET-CT parameters are attributable to the partial volume effect, relatively low FDG uptake by low-grade malignancies, and FDG uptake by benign entities. Nonetheless, PET-CT provides metabolic information, and hence,

combinations of PET-CT and other imaging modalities are expected to improve diagnostic accuracy for ALN metastasis in breast cancer, especially in TNBC.

The present study has several limitations that warrant consideration. First, the study is inherently limited by its retrospective design. Second, partial volume effects were not corrected. Third, CT morphological criteria were not included in the assessment of ALN status. Fourth, we were unable to match LNs evaluated by PET-CT and those that underwent pathologic examination. Instead, we assumed that the ALN assessed with the PET-CT criteria correlated with the overall pathologic diagnosis by surgical specimen.

In conclusion, the characteristics of SUV-T and SUV-LN differed according to the IHC subtype. Compared to other IHC subtypes, the true positivity of axillary metastasis on PET-CT was highest in the triple-negative subtype. These findings could help tailor the management for individual patients for therapeutic and diagnostic purposes.

## CONFLICT OF INTEREST

No potential conflict of interest relevant to this article was reported.

## REFERENCES

1. Fisher B, Bauer M, Wickerham DL, Redmond CK, Fisher ER, Cruz AB, et al. Relation of number of positive axillary nodes to the prognosis of patients with primary breast cancer: an NSABP update. *Cancer* 1983;52:1551-7.
2. Walls J, Boggis CR, Wilson M, Asbury DL, Roberts JV, Bundred NJ, et al. Treatment of the axilla in patients with screen-detected breast cancer. *Br J Surg* 1993;80:436-8.
3. Weiss RB, Woolf SH, Demakos E, Holland JF, Berry DA, Falkson G, et al. Natural history of more than 20 years of node-positive primary breast carcinoma treated with cyclophosphamide, methotrexate, and fluorouracil-based adjuvant chemotherapy: a study by the Cancer and Leukemia Group B. *J Clin Oncol* 2003;21:1825-35.
4. Arriagada R, Le MG, Dunant A, Tubiana M, Contesso G. Twenty-five years of follow-up in patients with operable breast carcinoma: correlation between clinicopathologic factors and the risk of death in each 5-year period. *Cancer* 2006;106:743-50.
5. Moffat FL Jr, Senofsky GM, Davis K, Clark KC, Robinson DS, Ketcham AS. Axillary node dissection for early breast cancer: some is good, but all is better. *J Surg Oncol* 1992;51:8-13.
6. Lucci A, McCall LM, Beitsch PD, Whitworth PW, Reintgen DS, Blumencranz PW, et al. Surgical complications associated with sentinel lymph node dissection (SLND) plus axillary lymph node dissection compared with SLND alone in the American College of Surgeons Oncology Group Trial Z0011. *J Clin Oncol* 2007;25:3657-63.
7. Noguchi M, Morioka E, Ohno Y, Noguchi M, Nakano Y, Kosaka T. The changing role of axillary lymph node dissection for breast cancer. *Breast Cancer* 2013;20:41-6.
8. Schwartz GF. Clinical practice guidelines for the use of axillary sentinel lymph node biopsy in carcinoma of the breast: current update. *Breast J* 2004;10:85-8.
9. Walsh R, Kornguth PJ, Soo MS, Bentley R, DeLong DM. Axillary lymph nodes: mammographic, pathologic, and clinical correlation. *AJR Am J Roentgenol* 1997;168:33-8.
10. Alvarez S, Anorbe E, Alcorta P, Lopez F, Alonso I, Cortes J. Role of sonography in the diagnosis of axillary lymph node metastases in breast cancer: a systematic review. *AJR Am J Roentgenol* 2006;186:1342-8.
11. Fuster D, Duch J, Paredes P, Velasco M, Munoz M, Santamaria G, et al. Preoperative staging of large primary breast cancer with [18F] fluorodeoxyglucose positron emission tomography/computed tomography compared with conventional imaging procedures. *J Clin Oncol* 2008;26:4746-51.
12. Eubank WB, Mankoff D, Bhattacharya M, Gralow J, Linden H, Ellis G, et al. Impact of FDG PET on defining the extent of disease and on the treatment of patients with recurrent or metastatic breast cancer. *AJR Am J Roentgenol* 2004;183:479-86.
13. Hatt M, Groheux D, Martineau A, Espie M, Hindie E, Giacchetti S, et al. Comparison between 18F-FDG PET image-derived indices for early prediction of response to neoadjuvant chemotherapy in breast cancer. *J Nucl Med* 2013;54:341-9.
14. Cerfolio RJ, Bryant AS. Ratio of the maximum standardized uptake value on FDG-PET of the mediastinal (N2) lymph nodes to the primary tumor may be a universal predictor of nodal malignancy in patients with nonsmall-cell lung cancer. *Ann Thorac Surg* 2007;83:1826-9.
15. Ueda S, Kondoh N, Tsuda H, Yamamoto S, Asakawa H, Fukatsu K, et al. Expression of centromere protein F (CENP-F) associated with higher FDG uptake on PET/CT, detected by cDNA microarray, predicts high-risk patients with primary breast cancer. *BMC Cancer* 2008;8:384.
16. Specht JM, Kurland BF, Montgomery SK, Dunnwald LK, Doot RK, Gralow JR, et al. Tumor metabolism and blood flow as assessed by positron emission tomography varies by tumor subtype in locally advanced breast cancer. *Clin Cancer Res* 2010;16:2803-10.
17. Levy L, Suissa M, Chiche JF, Teman G, Martin B. BIRADS ultrasonography. *Eur J Radiol* 2007;61:202-11.
18. Harvey JM, Clark GM, Osborne CK, Allred DC. Estrogen receptor status by immunohistochemistry is superior to the ligand-binding assay for predicting response to adjuvant endocrine therapy in breast cancer. *J Clin Oncol* 1999;17:1474-81.
19. Cheang MC, Chia SK, Voduc D, Gao D, Leung S, Snider J, et al.

- Ki67 index, HER2 status, and prognosis of patients with luminal B breast cancer. *J Natl Cancer Inst* 2009;101:736-50.
20. Veronesi U, Paganelli G, Viale G, Luini A, Zurrada S, Galimberti V, et al. A randomized comparison of sentinel-node biopsy with routine axillary dissection in breast cancer. *N Engl J Med* 2003;349:546-53.
  21. Jung J, Park H, Park J, Kim H. Accuracy of preoperative ultrasound and ultrasound-guided fine needle aspiration cytology for axillary staging in breast cancer. *ANZ J Surg* 2010;80:271-5.
  22. Goldhirsch A, Wood WC, Gelber RD, Coates AS, Thurlimann B, Senn HJ, et al. Progress and promise: highlights of the international expert consensus on the primary therapy of early breast cancer 2007. *Ann Oncol* 2007;18:1133-44.
  23. Goldhirsch A, Wood WC, Coates AS, Gelber RD, Thurlimann B, Senn HJ, et al. Strategies for subtypes-dealing with the diversity of breast cancer: highlights of the St. Gallen International Expert Consensus on the Primary Therapy of Early Breast Cancer 2011. *Ann Oncol* 2011;22:1736-47.
  24. Gianni L, Dafni U, Gelber RD, Azambuja E, Muehlbauer S, Goldhirsch A, et al. Treatment with trastuzumab for 1 year after adjuvant chemotherapy in patients with HER2-positive early breast cancer: a 4-year follow-up of a randomised controlled trial. *Lancet Oncol* 2011;12:236-44.
  25. Caudle AS, Yu TK, Tucker SL, Bedrosian I, Litton JK, Gonzalez-Angulo AM, et al. Local-regional control according to surrogate markers of breast cancer subtypes and response to neoadjuvant chemotherapy in breast cancer patients undergoing breast conserving therapy. *Breast Cancer Res* 2012;14:R83.
  26. Basu S, Chen W, Tchou J, Mavi A, Cermik T, Czerniecki B, et al. Comparison of triple-negative and estrogen receptor-positive/progesterone receptor-positive/HER2-negative breast carcinoma using quantitative fluorine-18 fluorodeoxyglucose/positron emission tomography imaging parameters: a potentially useful method for disease characterization. *Cancer* 2008;112:995-1000.
  27. Majid AS, de Paredes ES, Doherty RD, Sharma NR, Salvador X. Missed breast carcinoma: pitfalls and pearls. *Radiographics* 2003;23:881-95.
  28. Pamilo M, Soiva M, Lavast EM. Real-time ultrasound, axillary mammography, and clinical examination in the detection of axillary lymph node metastases in breast cancer patients. *J Ultrasound Med* 1989;8:115-20.
  29. Lernevall A. Imaging of axillary lymph nodes. *Acta Oncol* 2000;39:277-81.
  30. Luciani A, Itti E, Rahmouni A, Meignan M, Clement O. Lymph node imaging: basic principles. *Eur J Radiol* 2006;58:338-44.